Use of Landsat TM Digital Data for Estuarine Water Quality Modeling

Pedro Rios and Siamak Khorram
North Carolina State University
Raleigh, North Carolina, 27695-7106
U.S.A.

Robert C. Wrigley
National Aeronautics and Space Administration
Ames Research Center
Moffet Field, California 94035
U.S.A.

ABSTRACT

Landsat Thematic Mapper applicability for water quality modeling was tested on the San Francisco Bay-Delta. The approach involved simultaneous acquisition of TM data and 76 water surface measurements. Water samples were analyzed for chlorophyll a, turbidity and suspended solids. Linear regression models were developed between each of the water quality parameter measurements and Landsat digital data for 49 sample sites. The performances of these models were evaluated based on the application of the selected models to 20 additional sample sites and comparison of observed and predicted values for these sites. For each parameter, the applicability of a single model to the Bay, Delta and the entire study area was tested. Models were extended to the entire study area for the prediction of a parameter's spatial distribution over the entire San Francisco Bay and Delta. The results included a series of color coded maps, each pertaining to one of the water quality parameters, and statistical summaries. Areas of relatively high biological activity were clearly discernible in the Delta Entrapment Zone and center portions of the South Bay.

1.0 INTRODUCTION

Monitoring the spatial distribution of water quality parameters such as chlorophyll a, turbidity and suspended solids on estuarine waters is limited by temporal and spatial constraints. Temporal constraints that are commonly faced during measurements from boats include the inability to obtain a synoptic view of the dynamic and rapid changes in water conditions. Spatial constraints include estuary size and bathymetry. Consequently, interpolation between boat sampling stations on narrow channels, and extrapolation to broad shallow areas where boats cannot penetrate, are ineffective in terms of cost and accuracies.

Development of an effective water quality monitoring method on the San Francisco Bay estuary is necessary due to high economic, aesthetic and social pressures. Landsat Thematic Mapper (TM) repetitive coverage, improved spatial resolution and larger selection of bands represent a potential tool for mapping water quality parameters in estuarine systems on a repetitive basis.

The applicability of remote sensing digital data gathered from airborne and space platforms for water quality mapping has been studied on the San Francisco Bay estuary for nearly a decade. Khorram (1981a) used for the first time linear regression analysis to model chlorophyll a, suspended solids and turbidity on the northern reaches of the San Francisco Bay with airborne Ocean Color Scanner (OCS) acquired data. Landsat 3 repetitive coverage led to the use of the Multispectral Scanner (MSS) in an effort to map water quality over the Delta portion of the study area (Khorram, 1981b). Later, Landsat MSS-based models were developed for mapping water quality conditions throughout the entire San Francisco Bay and Delta (Khorram, 1985). The investigation hypothesized that TM digital data, with a narrower ranges of wavelength as opposed to MSS broad channels, could produce better modeling results. However, this series of studies using OCS and MSS data successfully located areas of high biological activity, called the "Entrapment Zone". The particulate matters in these areas are continously resupended after the oceanic water meets riverine water, which is the typical of partially-mixed estuaries.

The possibility of improving modeling results with the Thematic Mapper led to tests of how remotely sensed reflectance values from an airborne scanner similar to TM (Daedalus 1260 MSS) could be used to map surface chlorophyll a variations in the San Francisco Bay's shallow and turbid environment (Catts et al., 1985). Based on the results of this investigation, it was concluded that Landsat TM can potentially be used for water quality monitoring. In an effort to examine the applicability and consistency of relationships between chlorophyll a and simulated TM digital spectral data, Khorram et al. (1986) used simultaneously acquired airborne Daedalus MSS 1260 data and water quality samples in a multi-date analysis. This series of investigations confirmed that narrow ranges of wavebands which include the chlorophyll absorbtion and reflectance bands are more suited for modeling estuarine chlorophyll concentrations from remotely-sensed data.

Multispectral scanner data has been used by several investigators around the world for water quality modeling on coastal, inland, and estuarine ecosystems. Landsat MSS , airborne Daedalus 1260, the Coastal Zone Color Scanner (CZCS), and the Marine Ocean Color Scanner (MOCS) have been used successfully for mapping coastal water turbidity over several study areas (Munday and Alfoldi, 1979; Johnson et al., 1980; Tassan and Sturm, 1986; Collins and Pattiaratchi, 1984; Amos and Topliss, 1985; Campbell and Esaias, 1985; Lindell et al.,

1985; Dwivedi and Narain, 1987). More recently, Tassan (1987) proposed TM algorithms based on previously developed CZCS models for chlorophyll a and sediment concentrations with significant success. On inland water systems, Landsat MSS and TM data have been used successfully to model water quality parameters such as chlorophyll, secci depth, turbidity and suspended sediments (Carpenter and Carpenter, 1983; Verdin, 1985; Lathrop and Lillesand, 1986; Ritchie et al., 1987). On estuarine systems, Landsat MSS and TM data have been successfully used for displaying the spatial distribution of selected water quality parameters (Khorram and Cheshire, 1983, 1985; Stumpf, 1985). Enhanced spectral and spatial resolution of TM data with higher radiometric range, represent a clear advantage over Landsat MSS and a potential improvement on estuarine water quality modeling. Also, the Landsat TM repetitive and cost effective coverage when compared with similar multispectral data, may indicate its applicabilty as a cost-effective and practical alternative for assessing water quality conditions on a repetitive basis for water resource managers.

2.0 STUDY AREA

The San Francisco estuarine system is a complex of embayments, sloughs, marshes and rivers. The system is the largest coastal embayment of the Pacific Coast of the U.S. The relative shallow Bay (average depth of 6 m. at mean lower low water) is characterized by broad shallows (2 - 6 m. deep) incised by narrow channels (10 - 20 m deep) with a mean annual flow of 600 m^3/sec. (Conomos et al., 1985). This estuary is comprised of two hydrologically distinct areas. The Northern reach (Delta) is a partially mixed estuary with seasonally varying river inflow. The Southern reach (Bay) is a tidally-oscillating lagoon-type estuary (Conomos et al., 1985). While river inflow brings dissolved and suspended particulate matter into the system, the tidal currents mix the water column and determine circulation patterns. The resultant system's circulations when combined with wind induced waves cause the suspension of sediments from shallow bottom parts of the bay into the system.

The salt-induced density difference between marine and riverine waters causes a characteristic two-layered flow. A surface low density layer (river derived) flows seaward over a bottom high density layer (ocean derived) that flows landward. When riverine fresh water meets saline waters a null zone with a tidally-averaged bottom current of zero velocity and greater vertical density gradient develops. This null flow combined with a salinity enhanced floculation of suspended inorganic and organic materials causes retention of particles within the circulation cell: the "Entrapment Zone".

3.0 OBJECTIVES

The objectives of this study were : (1) to determine the usefulness of Landsat-TM digital data for modeling chlorophyll a, turbidity and suspended solids on estuarine environments when combined with simultaneous surface measurements from boats; and (2) to determine whether a single TM-based model can be developed to be applicable to both the Delta and the Bay portion of the San Francisco Bay/Delta.

4.0 SELECTION OF BANDS, RATIOS OR COMBINATIONS USED AS INDEPENDENT VARIABLES

Selection of the models' independent variables was based on the bio-optical properties of water and previous similar remote sensing investigations. Investigators have experienced two distinct distributions of water quality parameters over the Bay and Delta portions of the study area (Khorram and Pelkey, 1987). Using Landsat MSS data, Pelky (1986) demonstrated the usefulness of regional based models that can recognize the characteristics of certain water quality parameters in these two distinct regions. It was this line of reasoning that lead to preliminary data analysis for the Bay area separate from the Delta area. We expected that the bio-optical properties of the Bay and Delta sub-estuaries would differ due to the different sources of upwelling radiance on these areas. Four sources of upwelling radiance have been identified as the major influence on the inherent properties of ocean color. These sources are: (1) live phytoplankton; (2) associated biogenous and dissolved detritus; (3) terrigenous particles and resuspended sediment; and (4) dissolved terrigenous and anthropogenic organic matter, Gelbstoff, or yellow substance (Sathyendranath and Morel, 1983). Researchers (i.e., Morel and Prieur, 1977) have separated oceanic waters, whose bio-optical properties are dominated by phytoplankton and their byproducts (Case 1 Waters) from those waters in which resuspended sediments, terrigenous particles, dissolved organic matter (terrigenous yellow substance) or anthropogenic influx are present (Case 2 Waters). The Case 2 waters can be classified as "sediment-dominated" or "yellow-substance-dominated" depending on the location and sources of terrigenous influxes and the seasonal water conditions. While the Delta waters tend to be dominated by resuspended sediments and terrigenous particles (sediment-dominated Case 2 waters), the Bay waters tend to be dominated by terrigenous yellow substance and dissolved organic matter derived from algae and detritus (yellow-substance dominated Case-2 waters). Consequently, different behavior between the San Francisco Bay and Delta optical properties was expected. Contrary to expectations, analysis indicated that models based on the entire study area could perform as well or better than regional Bay or Delta models. In subsequent analyses, data from the Bay and Delta were examined both separately and combined to determine if the selected independent variables would adequately account for conditions over the entire system. Also, it was more desirable if a

single model would adequately represent the water quality distributions over the entire study area. For these reasons, Bay and Delta portions were both treated separately and also combined for model development and evaluation. As mentioned earlier, the models performed just as well or better when applied to the entire study area.

4.1 Chlorophyll *a* model variables.

In the sediment-dominated as well as yellow-substance dominated Case-2 waters, the reflectance values should indicate better differentiation of chlorophyll *a* concentrations in the regions from 400 to 500 nm and 660 to 690 nm (Gower et al., 1984). These spectral regions correspond, approximately, to TM band 1 (450 to 520 nm) and TM band 3 (630 to 690 nm). Studies of various laboratory grown phytoplankton species demonstrated peaks of absorption centered at 440 nm and 675 nm with depressed scattering (Morel, 1980). The variability of optical properties occurs due to chlorophyll-detritus absorption and its associated cellular scattering. While the energy absorbed is a measure of energy lost, this energy is used for primary productivity which causes backscattering changes in the plankton's cellular material. By using TM band 1 (TM1), it was expected that the upwelling radiance would decrease as chlorophyll *a* concentrations increase. The atmospheric haze contributions are to be expected in TM band 1 (TM1); inspection of the study scene lead to the assumption that local atmospheric composition was horizontally uniform. In order to account for signal contributions on the red portions of the spectrum, TM band 3 (TM3) was proposed as a model variable. At 630-690 nm, radiance values from clear water are low and a characteristic peak in reflectance at 675 nm is typically observed due to natural illumination induced fluorescence (Neville and Gower, 1977; Wilson and Kiefer, 1979; Morel, 1980; Gower et al., 1984). These factors combined with the lack of strong atmospheric absorption in the 685 (+/- 10 nm) spectral region suggested the use of TM3 as a model variable. At high chlorophyll *a* levels, the amount of energy absorbed by the sensor increases as the chlorophyll values increase.

4.2 Turbidity model variables.

In Case-2 waters where sediment and chlorophyll distributions appear to be uncorrelated, associations between turbidity measurements and remotely-sensed spectral data should account for sediment levels versus plankton induced turbidity. Laboratory and *in situ* studies of upwelling radiance on turbid waters consistently show increasing energy fluxes from the blue wavelengths (400 nm) to a peak in the region between 500 and 600 nm, with a relative decrease on the 600 to 700 nm region (More, 1980; Fisher, 1984; Mckin et al., 1984). Suspended silt and clay spectral signatures show a greater rate of increase in the backscattered flux in the red relative to the green parts of the spectrum. A difference term, TM band 2 (510-600 nm) and TM band 3 (630-690 nm) was used to detect

changes in upwelling radiances caused by suspended sediment. As sediments levels increase, it was expected that the "difference term" would increase due to a relatively higher increase of reflected energy in the red part of the spectrum (TM3). In order to account for chlorophyll *a* derived detritus and yellow substance, the spectral influence of a ratio of TM1 to TM2 was tested as an additional part of the predictor variable. This ratio (which corresponds to chlorophyll *a* maximum and minimum absorptions levels) is combined with the difference term to account for variations in turbidity not accounted by the difference term (TM3 - TM2) alone. A similar model has been developed for the Coastal Zone Color Scanner (Tassan, 1984, 1986). Thus, the ratio when multiplied by the difference term can describe estuarine turbidity by considering chlorophyll *a*, terrigenous particles, resuspended sediments, dissolved organic matter and anthropogenic influx influences on a spectral signature detected by TM.

4.3 Suspended solids model variables.

Organic and inorganic suspended materials alter the inherent reflectance of water mixtures. Laboratory and *in situ* investigations show an increase in the backscattered energy flux in the near-infrared wavelengths as silt-clay concentrations increase (More, 1980; Yentsch, 1983; Mckin et al.,1984). On the other hand, similar studies indicate that organic matter produced by soil leaching and biological material decomposition reduces the water reflectance in the region between 420-720 nm (Bricaud et al. 1981; Wittie et al., 1982). For these reasons, ratios of TM band 2 to TM band 4 (760-790 nm) and TM band3 to TM band 5 (1550-1750 nm) are proposed as model variables. It is expected that as the suspended solids concentrations vary these ratios of visible to infrared light can detect surface variations due to influences of both organic and inorganic matter.

5.0 RESEARCH METHODS

Research methods used in this study involved: (i) acquisition of near surface ($\leq$ 1 foot) water samples from boats simulataneous with Landsat TM data, (ii) extraction of digital count values corresponding to the sample site from computer compatible tapes, (iii) laboratory analysis of the water samples taken from 69 sites, (iv) development of linear models relating TM data to surface water quality measurements, and (v) application of regression equations to the entire study area to produce a series of color-coded maps each displaying the spatial distribution of a water quality parameter of interest.

5.1 Water sample collection and laboratory analysis.

On May 2, 1984, samples were collected from boats at 76 sample sites throughout South Bay, San Pablo Bay and Delta areas. Seven sites were later eliminated since they were located outside the Landsat scene. All samples were collected within 11

minutes before and 85 minutes after the exact time of satellite overpass time at 10:30 AM, Pacific Daylight time. Chlorophyll a samples were glass fiber filtered, extracted with acetone and measured for fluorescence levels. These levels were converted to chlorop concentrations in ug/l. Turbidity tests were done with a Horizon turbidimeter and reported in Nephelometric Turbidity Units (NTU). Suspended solids samples were filtered, dried, weighted and concentrations expressed in mg.

5.2 Acquisition and processing of Landsat TM data.

A Landsat TM scene covering the study area was obtained from NASA-Ames Research Center in the form of computer compatible tapes. The Thematic Mapper records six channels of visible and infrared reflected energy at 30 m resolution and one channel of thermal energy at 120 m resolution (Table 1). Tapes were processed at the Computer Graphics Center, North Carolina State University using Image Analysis System (IAS) software.

Location of sample sites (latitude/longitude) was determined from NOAA nautical charts. These locations were transformed to image coordinates, and were visually inspected for accuracy as well as for cloud cover or any obstructing feature. For all visible and reflective infrared bands, digital count values for the sample site as well as the surrounding 3 by 3 pixel block were extracted. Averages of the 3 by 3 block were computed and used for model development in order to minimize errors in locating the sample sites. None of the pixel block averages differed significantly from its corresponding single pixel value in the center of the block.

5.3 Model Development.

Linear regression analysis was used in an effort to determine associations between water quality parameters and the selected TM bands, either alone or as a linear combinations or ratios . Twenty sample sites were selected at random from the entire data set (n=69), held out from model development, and used for verification of the models developed using the remaining 49 sites (Figure 1). Criteria for model evaluation included R-square values, F-test results for linear model adequacy, t-test results of regression coefficient significance, standard errors of each coefficient and the overall model, model complexity, and residual analysis.

5.4 Model application to the entire study area.

Image files corresponding to the study area were generated for all TM visible and reflective infrared bands. These image files were then masked by using TM band 5 as the source for distinguishing the land/water interface. Linear equations were applied on a pixel-by-pixel basis to the entire study area in order to create files representing the distribution of concentrations of the parameter of interest. Discrete, meaningful classes were created and color-coded for the

generation of chlorophyll a, turbidity and suspended solids maps.

6.0 RESULTS AND DISCUSSION

Results of this research include: (i) a record of the measured values of water quality parameters and digital count values for 69 sample sites; (ii) a series of mathematical models for predicting water quality parameters of interest; (iii) statistical summaries of the modeling and verification results; and (iv) a series of color coded maps that display water quality parameters distributions throughout the entire study area.

Results of surface water measurements and extracted digital count values are presented in Table 2. Predictive mathematical models are listed below:

Chlorophyll a model

$$\text{Chl-a (ug/l)} = 32.14 - 0.66(TM1) + 1.14(TM3),$$

Turbidity model

$$\text{Tur (NTU)} = 47.07 - 2.00(X1),$$

$$X1 = (TM2 - TM3)*(TM1/TM2)$$

Suspended Solids

$$\text{Sus. (mg/l)} = 7.53 - 2.62(X1) + 1.44(X2),$$

$$X1 = (TM2/TM4),$$

$$X2 = (TM3/TM5).$$

In all of the models, TM1, TM2, TM3, TM4, and TM5 represent the digital count values in bands 1, 2, 3, 4, and 5 of TM data respectively.

A summary of statistical modeling and verification results is presented in Table 3. Plots of predicted vs. observed values and residuals vs. predicted values for modeling and verification data sets are show in Figures 2, 3, 4. The predicted versus observed value plots show how well the linear equations fitted the data. The residuals versus predicted values plots show the distribution of residuals around the zero axis for the predicted range of values. A random distribution of residuals around the zero axis indicates homogeneous variance of the residuals. All F values were statistically significant at the 5 % level. Coefficients of determination (R-square) varied from medium for suspended solids (R^2=.49) and chlorophyll a (R^2=.62) to high for turbidity (R^2=.74). The medium R-square values for the chlorophyll model may be due to sediment influence represented on TM3. The high sediment

concentrations reduce model sensitivity to high chlorophyll a levels, a condition that can be observed on greater residuals of higher predicted values in the residuals vs. predicted value plot (Figure 2c). The relatively low R-square value for the suspended solids model may be due to the lack of model sensitivity over the conditions in the Bay portion of the study area. Suspended solids maximums on the Delta can be characterized by the variables for suspended sediment ratios : TM2/TM4 and TM3/TM5 indicating high sediments levels in the Delta. During summer, high levels of suspended solids commonly found at the southern boundary of the Bay may be due to local streams and sewage discharges. Low levels at the north boundary may be due to low Delta inflow into the Bay. The northern region of the Bay acts as a dilution zone (sink) when ocean waters enter the estuary. The gradient between the northern and southern extremes of the South Bay results in a net suspended sediment diffusion northward and a lack of sediment retention in the Bay (Conomos et al., 1979). This condition results in low suspended sediments and very low infrared reflectance (perhaps to low to be detected by TM) at sample points located in the Bay. Successful mapping of suspended solids on the Bay portions of the study area with ratios of visible to infrared bands may be limited due to low suspended solids levels typical of the spring-summer season.

Color-coded water quality maps for chlorophyll a , turbidity, and suspended solids are shown in Figures 5. In these figures, the values of water quality parameters increase with color changes from blue to green to yellow to orange to red. That is blue represents the lowest value and red represents the highest value. Results of the chlorophyll a map coincide with surface measurements from boats. Location of a well defined Entrapment Zone in Suisun Bay coincides with the summer periods of low river fresh water inflow and rapid neritic and estuarine planktonic species growth (Cloern, 1979, Cloern and Nichols, 1985). Also, the observed values on the TM data over the shallow parts of San Pablo Bay have been identified as the location of the water mixing zones at the mouths of Petaluma and Sonoma Creeks during this time of the year. Minimum values at South Bay coincide with the seasonal isohaline conditions during which rapid consumption of plankton by benthic fauna occurs due to the high water residence times resulting from low local stream outflows (Cloern et al., 1983).

Turbidity distributions show a maximum zone on the Delta, a minimum zone on Central Bay and increasing concentration gradients southward on South Bay. High turbidity values in Grizzly and Honker Bays indicate the aereal extent of the turbid Entrapment Zone resulting from landwardly transported sediments during summer flow conditions. When riverine waters meet saline waters a null zone with a tidally averaged bottom current velocity of near zero and greater vertical gradients develops. This null flow combined with salinity enhanced floculation of suspended inorganic particles into aggregates causes faster settling rates for the aggregated materials.

These aggregated materials are transported downstream or settle into the lower flow layer (moving landwardly) which accumulates at the upstream end of the freshwater-saltwater mixing zone - the Entrapment Zone (Arthur and Ball, 1979). The results of our TM-based models are in close agreement with reported values through conventional survey methods as well as other remote sensing investigation over this study area. (Arthur and Ball, 1979; Cloern and Nichols, 1985, Conomos et al., 1985; Khorram, 1981, 1985).

Suspended solids models suffer from the expected lack of model sensitivity over the Bay region. While a turbid Entrapment Zone in the Delta is recognized, the observed feature over the South Bay region is the gradient from deep channels to shoal areas. High concentration levels observed over the South Bay deep channels not only agree with conventional survey methods results but also confirm the fact that the suspended solids model using visible to infrared wavelength ratios is applicable to areas of high parameter concentrations. It is at high concentrations that the natural water infrared absorption rate is altered.

7.0 CONCLUSIONS

Conclusions derived from this investigation include:

1. Landsat TM digital data can be successfully applied for estuarine water quality modeling. Chlorophyll a, turbidity and suspended solids models have been developed for displaying their spatial distributions over the entire San Francisco Bay/Delta.

2. The higher spatial and spectral resolution of TM proved more useful than Landsat MSS data for water quality mapping over this complex estuary.

3. Better or equally good results were achieved when a model was developed for the entire study area, versus one for the Bay and one for the Delta.

4. TM bands 1 and 3 contained most of the information needed for chlorophyll a modeling. These bands when used in linear regression analysis, can identify areas of high biological, chemical and physical activity on the Delta Entrapment Zone as well as its migration to shallow portions of San Pablo Bay.

5. A combination variable of the form : TM band 2 minus TM band 3, multiplied by the ratio of TM band 1 to TM band 2 contains information about the lithogenous and biogenous induced turbidity on estuarine waters. This band combination can be used in linear regression analysis for the prediction of turbidity values on the Delta as well as Bay area.

6. The ratios of TM band 2 to TM band 4 and TM band 3 to TM band 5 can be used as independent varibles for prediction of high suspended solids. The observed model's lack of sensitivity over the Bay portions of the study area as opposed to the Delta area indicates that visible to infrared wavelength ratios cannot depict typical low flow summer conditions.

7. Multi-date studies are recommended to test the proposed general form of the models, especially the suspended solids model which behaved poorly at the low levels within the study date.

8. Repetitive coverage and less expensive nature of TM data makes this scanner more suitable and more practical for water quality modeling as compared with commonly available aircraft multispectral data or Landsat MSS data.

ACKNOWLEDGEMENTS

The authors would like to thank Dr. Allen Knight of the University of California at Davis for the coordination of water quality sampling and the laboratory analysis of water quality samples, Dr. James Cloern of the Water Resources Division of the U.S.G.S. for the collection and analysis of water quality samples from the South San Francisco Bay and providing major inputs to the modeling of water quality parameters. We also would like to thank Dr. Mike Aldridge of NOAA-Nation Marine Fisheries Service in Tiburon and Mr. Harlan Proctor of the California Dept. of Water Resources for their contribution in collecting water quality samples. Thanks are also extended to Dr. William Hafley and Dr. James Gregory of North Carolina State University for their comments and inputs in the documentation of the research discussed in this manuscript.

REFERENCES

Amos, C.L. and B.J. Topliss, 1985, Discrimination of suspended particulate matter in the Bay of Fundy using the Nimbus 7 Coastal Zone Color Scanner. Canadian J. of Remote Sensing, 11(1), pp. 85-92.

Arthur, J.F. and M.D. Ball, 1979, Factors influencing the entrapment of suspended material in the San Francisco Bay-Delta estuary. In **San Francisco Bay: The Urbanized Estuary**, edited by T.J. Conomos (American Association for the Advancement of Science), pp. 143-174.

Bricaud, A.; Morel, A. and L. Prieur, 1981, Absorption by dissolved organic matter of the sea (yellow substance) in the uv and visible domains. Limnol. Oceanogr., 26(1), pp. 43-53.

Campbell, J.W. and W.E. Esaias, 1985, Spatial patterns in temperature and chlorophyll on Nantucket Shoals from airborne remote sensing data, May 7-9, 1981. J. of Marine Res., 43, pp. 139-161.

Carpenter, D.J. and S.M. Carpenter, 1983, Modeling inland water quality using Landsat data. Remote Sensing of the Env., 13, pp. 345-352.

Catts, G.P.; Khorram, S.; Cloern, J.E.; Knight, A.W. and S.D. Degloria, 1985, Remote sensing of tidal chlorophyll-a variations in estuaries. Int. J. Remote Sensing, 6(11), pp. 1685-1706.

Cloern, J.E., 1979, Phytoplakton ecology of the San Francisco Bay system: the status of our current understanding. In **San Francisco Bay: The Urbanized Estuary**, edited by T.J. Conomos (American Association for the Advancement of Science), pp. 247-264.

Cloern, J.E.; Alpine, A.E.; Cole,B.E.; Wong, R.L.J.; Arthur, J.F. and M.D. Ball, 1983, River discharge controls phytoplankton dynamics in the northern San Francisco Bay estuary. Estuarine, Coastal and Shelf Sci., 16, pp. 415-429.

Cloern, J.E. and F.H. Nichols, 1985, Time scale and mechanisms of estuarine variabilty, a synthesis from studies of San Francisco Bay. Hydrobiologia, 129, pp. 229-237.

Collins, M. and C. Pattiaratchi, 1984, Identification of suspended sediment in coastal waters using airborne thematic mapper data, Int. J. Remote Sensing, 5(4), pp. 635-657.

Conomos, T.J. 1979, Properties and circulations of San Francisco Bay waters. In **San Francisco Bay: The Urbanized estuay**, edited by T.J. Conomos (American Association for the Advancement of Science), pp.47-84.

Conomos, T.J.; Smith R.E. and J.W. Gartner, 1985, Environmental setting of San Francisco Bay. Hydrobiologia, 129, pp. 1-12.

Conomos, T.J.; Smith, R.E. Peterson, D.H. Hager, S.W.; and L.E. Schemel, 1979, Process affecting seasonal distribution of water properties in the San Francisco bay estuary system. In **San Francisco Bay: The Urbanized Estuary**, edited by T.J. Conomos (American association for the Advancement of Science), pp. 115-142.

Dwivedi, R.M. and A. Narain, 1987, Remote sensing of phytoplankton - An attempt from Landsat Thematic Mapper. Int. J. Remote Sensing, 8(10), pp. 1563-1569.

Fischer, J. and P. Koepke, 1984, The influence of perturbing water properties in chlorophyll mapping. Proceedings of IGARSS '84 Symposium, Strabourg, France, pp. 709-713.

Gower, J.R.F.; Lin, S. and G.A. Borstad, 1984, The information content of different optical spectral ranges for chlorophyll estimation in coastal waters. Int. J. Remote Sensing, 5(2), pp. 349-364.

Johnson, R.W. and R.C. Harris, 1980, Remote Sensing for water quality and biological measurements in coastal waters. Photogramm. Eng. Remote Sensing, 46(1), pp. 77-85.

Khorram, S., 1981a, The use of Ocean Color Scanner data in water quality mapping. Phtogramm. Eng. Remote Sensing, 47(5), pp. 667-676.

Khorram, S., 1981b, Water quality mapping from Landsat digital data. Int. J. Remote Sensing, 2(2), pp.145-153.

Khorram, S., 1985, Development of water quality models applicable throughout the entire San Francisco Bay and Delta. Photogramm. Eng. Remote Sensing, 51(1), pp. 53-62.

Khorram, S.; Catts, G.P.; Cloern, J.E. and A.W. Knight, 1986, Modelling of estuarine chlorophyll from an airborne scanner. Proceedings of IGARSS '86 Symposium, Zurich, Switzerland, pp. 1387-1396.

Khorram, S. and H. Cheshire, 1983, The use of Landsat MSS digital data in water quality mapping of the Neuse river estuary, N. C.. Water Res. Inst. of Univ. of N.C., report no. 193, pp. 1-29.

Khorram, S. and H. Cheshire, 1985, Remote sensing of water quality in the Neuse River estuary, North Carolina. Photgramm. Eng. Remote Sensing, 51(3), pp. 329-341.

Khorram, S. and P.D. Pelkey, 1987, Development of multidate estuarine water quality models using Landsat 2 and 4 MSS data. In **Technical Papers ASPRS-ACSM Annual Convention**, Baltimore, Ma., vol. 1, pp. 1-26.

Lathrop, R.G. and T.M. Lillesand, 1986, Use of Thematic Mapper data to assess water quality in the Green Bay and Central Lake, Michigan. Photogramm. Eng. Remote Sensing, 52(5), pp. 671-680.

Lindell, L.T.; Steinvall, O.; Jonsson, M.; and TH. Claesson, 1985, Mapping of coastal-water turbidity using Landsat imagery. Int. J. Remote Sensing, 6(5), pp. 629-642.

Mckin, H.L.; Mercy, C.J. and R.W. Layman, 1984, Water quality monitoring using an airborne spectroradiometer. Photogramm. Eng. Remote Sensing, 50(3), pp. 353-360.

Moore, G.K., 1980, Satellite remote sensing of water turbidity. Hydrological Sciences Bulletin, 25(4), pp. 407-421.

Morel, A., 1980, In-water and remote measurement of ocean colour. Boundary-Layer Meteorol., 18, pp. 177-201.

Morel, A. and L. Prieur, 1977, Analysis of variations in ocean color. Limnol Oceanogr., 22(4), pp. 709-722.

Munday, J.C. and T.T. Alfoldi, 1979, Landsat test of diffuse reflectance models for aquatic suspended solids measurements. Remote Sensing of Env., 8, pp. 169-183.

Neville, R. A. and J.F.R. Gower, 1977, Passive remote sensing of phytoplankton via chlorophyll-alpha fluorescence. J. of Geophy. Res., 82(24), pp. 3487-3493.

Pelkey, P.D., 1986, Multidate analysis of remotely-sensed estuarine water quality parameters using Landsat MSS. M.S. Thesis, North Carolina State University, pp. 1-88.

Ritchie, J.C.; Cooper, C.M. and J. Yoingqing, 1987, Using Landsat Multispectral Scanner data to estimate suspended solids in Moon Lake, Mississippi. Remote Sensing of Env., 23, pp. 65-81.

Sathyendranath, S. and A. Morel, 1983, Light emerging from the sea - interpretation and uses in remote sensing. In **Remote Sensing Applications in Marine Science and Technology**, edited by A.P. Cracknell (D. Reidel Pub. Co.), NATO ASI series # 106, pp. 323-357.

Stumpf, R.P., 1985, Physical interpretation of estuarine water color using vector analysis of satellite data. Proceedings of IGARSS '85, vol. 2, Amherst, Mass., pp. 971-974.

Tassan, S., 1984, A method for the retrieval of phytoplankton and suspended sediment concentrations from remote measurements of water colour. Proceedings of the 15th International Symposium on Remote Sensing of the Environment, Ann Arbor, Michigan, pp. 577-586.

Tassan, S., 1987, Evaluation of the potential of the Thematic Mapper for marine application. Int. J. Remote Sensing, 8(10), pp. 1455-1478.

Tassan, S. and B. Sturm, 1986, An algorithm for the retrieval of sediment content in turbid costal waters from CZCS data. Int. J. Remote Sensing, 7(5), pp. 643-655.

Verdin, J.P., 1985, Monitoring water quality conditions in a large western reservoir with Landsat imagery. Photgramm. Eng. Remote Sensing, 51(3), pp.343-353.

Wilson, W.H. and D.A. Kiefer, 1979, Reflectance spectroscopy of marine phytoplankton. Part 2. A simple model of ocean color. Limnol. Oceanogr., 24(4), pp. 673-682.

Wittie, W.G.; Whitlock, C.H.; Harris, R.C.; Usry, L.R.; Poole, L.R.; Houghton, W.M.; Morris, W.D. and E.A. Guiganus, 1982, Influence of dissolved organic matter on turbid water optical properties and remote sensing reflectance. J. Geophy. Res., 87(C1), pp. 441-446.

Yentsch, C.S., 1983, Remote sensing of biological substances. In **Remote Sensing Applications in Marine Science and Technology**, edited by A.P. Cracknell (D. Reidel Pub. Co.), NATO ASI series # 106, pp. 263-297.

Table 1. Landsat-TM, channel wavelength ranges.

Channel	Wavelength(nm)	Color
1	450 - 520	Blue
2	510 - 600	Green
3	630 - 690	Red
4	760 - 790	Infrared
5	1550 - 1750	Infrared
7	2080 - 2350	Infrared
6	10.40 - 12.60 (K)	Thermal Infrared

Table 2. Chlorophyll a (ug/l), turbidity (NTU) and suspended solids (mg) near-surface measurements, and corresponding digital count values for 76 sites on May 2, 1984.

SITE	TIME	OBSERVED CHLOROPHYLL	OBSERVED TURBIDITY	OBSERVED SUSPENDED SOLIDS	TM CHANNEL 1	TM CHANNEL 2	TM CHANNEL 3	TM CHANNEL 4	TM CHANNEL 5
3	10:30	4.80	41.50	6.75	104.22	40.00	37.44	14.44	10.67
4	10:40	4.04	34.50	4.49	105.78	43.56	42.33	14.56	9.44
5	10:50	5.00	34.10	6.08	106.56	43.33	41.78	14.33	9.44
6	11:00	5.38	19.00	3.74	107.22	43.89	39.78	14.44	10.33
7	11:10	5.57	26.00	5.70	115.22	47.00	45.56	17.11	15.44
8	11:20	7.11	22.30	4.58	109.33	45.11	42.56	14.44	10.11
9	11:30	5.76	31.00	6.40	107.67	43.22	41.00	14.00	9.44
10	11:40	5.76	38.50	7.15	110.44	43.78	41.78	15.33	15.78
12	11:36	3.65	29.30	8.27	109.67	44.89	46.33	17.56	9.33
13	11:28	3.46	25.10	7.40	106.11	42.78	40.22	14.22	9.00
14	11:20	4.04	17.50	6.33	104.89	40.89	34.78	13.78	10.33
15	11:11	3.46	12.60	4.56	101.00	38.22	30.44	10.44	7.00
16	11:05	3.65	15.30	5.35	99.67	36.33	29.44	10.22	7.56
17	11:00	3.46	10.50	5.65	100.78	37.33	30.89	10.78	8.44
18	10:51	3.46	14.30	5.65	101.44	38.44	31.33	12.33	7.67
19	10:40	2.88	15.80	5.00	102.44	38.00	31.11	11.44	8.11
20	10:35	1.92	13.00	5.21	103.11	40.11	33.11	11.44	6.89
21	10:30	1.92	17.00	4.16	104.11	40.78	34.11	12.56	7.22
22	10:25	3.84	12.80	5.02	103.44	37.00	29.33	11.33	9.33
23	10:39	3.84	10.10	4.50	98.78	36.00	28.22	11.22	7.00
24	10:48	3.84	9.00	3.50	101.44	37.78	29.78	12.67	8.00
25	10:55	4.04	14.50	7.12	98.33	34.67	27.33	10.33	7.33
26	11:08	4.80	7.80	4.81	107.00	39.22	32.33	15.22	12.56
27	11:18	4.80	8.50	5.08	97.78	34.11	25.62	11.17	8.95
28	11:30	1.39	6.00	4.29	96.72	34.89	24.89	10.89	6.84
29	11:47	3.46	7.10	5.10	95.67	33.22	23.56	10.33	8.00
33	10:37	5.19	17.30	5.36	116.11	46.89	42.00	16.89	16.67
34	10:44	10.57	24.80	5.78	108.11	43.67	37.78	12.00	7.33
35	10:51	14.00	22.40	6.22	103.00	41.78	39.22	13.44	7.78
36	11:05	19.00	47.80	7.96	102.89	41.67	38.67	11.33	5.89
37	11:14	10.18	26.10	5.75	104.67	43.22	41.56	11.44	5.44
38	11:22	13.64	37.50	5.45	105.44	43.22	41.00	12.78	6.33
39	11:34	15.18	65.80	8.51	104.56	44.00	43.78	14.44	7.67
40	11:44	21.13	45.80	7.53	105.56	45.00	48.22	17.78	7.00
41	11:54	33.82	65.45	8.33	105.00	45.11	48.44	19.11	9.00
42	12:08	35.55	78.40	9.94	109.44	47.67	53.00	23.33	12.22
43	12:15	32.67	85.50	10.58	108.78	47.11	54.78	27.11	10.89
44	12:25	50.00	100.00	12.68	111.22	48.67	57.78	29.11	11.22
45	10:30	31.13	110.00	13.29	106.22	45.78	51.11	22.44	9.33
46	10:38	27.86	110.30	13.73	107.78	47.44	54.89	25.00	9.89
47	10:44	32.67	121.30	15.57	106.22	46.44	53.33	24.33	8.56
48	10:49	37.47	106.30	11.04	109.78	47.44	54.33	24.11	11.67
49	10:57	20.18	70.00	8.71	109.67	47.78	53.67	23.11	12.11
50	11:02	25.94	79.50	9.45	111.11	48.22	53.67	23.89	13.33
51	11:10	16.33	69.00	8.41	111.44	48.22	53.67	23.67	13.11
52	11:17	18.45	60.00	6.02	112.00	48.78	54.89	24.22	14.44
53	11:25	18.25	61.50	7.96	109.44	47.00	51.44	23.22	16.33
54	11:30	20.18	47.30	5.60	108.11	46.11	51.33	22.22	13.56
55	11:37	16.72	45.50	5.34	109.44	45.67	50.22	22.44	14.89
57	10:56	24.98	107.70	13.09	110.11	48.22	54.56	23.78	9.67
58	11:07	39.39	120.00	14.14	114.00	50.33	58.67	25.44	11.56
59	11:16	18.25	70.50	8.06	108.89	46.33	50.67	21.00	9.67
60	11:20	27.86	99.00	11.22	163.22	72.22	88.11	51.11	67.78
61	11:25	13.45	60.50	6.21	108.67	47.33	54.78	26.89	10.00

SITE	TIME	OBSERVED CHLOROPHYLL	OBSERVED TURBIDITY	OBSERVED SUSPENDED SOLIDS	TM CHANNEL 1	TM CHANNEL 2	TM CHANNEL 3	TM CHANNEL 4	TM CHANNEL 5
62	11:31	31.70	117.50	14.40	109.78	47.44	54.78	27.78	11.22
63	11:37	20.18	125.00	14.90	109.89	47.33	55.78	28.33	11.78
64	11:44	18.25	82.20	9.99	109.89	48.11	54.67	25.67	13.33
65	11:49	18.06	65.00	6.86	109.78	48.56	54.67	23.33	10.33
66	11:55	15.76	62.30	6.49	109.00	47.67	55.11	23.89	11.11
67	10:19	16.33	36.00	3.83	107.00	45.11	47.56	20.11	14.56
68	10:29	12.49	28.10	3.25	106.89	45.11	47.11	20.56	15.00
69	10:34	5.76	30.10	2.56	104.67	44.78	44.33	19.22	13.33
70	10:41	8.45	24.50	2.24	105.44	44.56	43.78	19.00	14.56
71	10:51	8.45	19.00	1.89	91.78	41.22	40.17	17.28	11.39
72	10:59	5.38	23.00	2.43	104.67	44.44	43.78	18.44	14.33
73	11:05	3.84	26.60	2.98	104.56	44.22	43.33	17.89	12.67
74	11:11	2.50	19.00	1.96	106.22	44.78	44.33	19.11	14.44
75	11:17	3.46	20.00	1.91	107.67	44.89	44.44	19.11	15.11
76	11:22	3.84	22.50	2.14	103.22	42.22	41.67	16.44	10.44

Table 3. Summary of chlorophyll a, turbidity, suspended solids modeling and verification results.

Model	R^2	F / Prob>F	R.M.S. error	Regression Coefficient	Coefficients Standard Errors	Prob> |T|
Chl.a modeling (n=49)	.62	37.78 / .0001	7.25	a=34.14 b= 0.66 c= 1.14	29.35 0.32 0.16	.2508 .0467 .0001
Chl.a verifying (n=20)	.62	13.88 / .0003	7.54	a=36.78 b= 0.73 c= 1.26	19.67 0.27 0.27	.0788 .0143 .0002
Tur. modeling (n=49)	.74	131.89 / .0001	17.76	a=47.07 b= 2.00	2.55 0.17	.0001 .0001
Tur. verifying (n=49)	.74	51.49 / .0001	18.91	a=45.52 b= 2.14	4.24 0.30	.0001 .0001
TSS. modeling (n=20)	.49	21.69 / .0001	2.51	a= 7.53 b= 2.62 c= 1.44	3.38 4.40 4.38	.0015 .0001 .0001
TSS. verifying (n=20)	.52	9.06 / .0021	2.56	a=10.53 b= 4.03 c= 1.59	2.64 1.02 0.50	.0010 .0010 .0059

Models of the forms: Chl a(ug/l) = a + b(X1) + c(X2), where X1 is TM channel 1 and X2 is TM channel 2; Tur(NTU) = a + b(X1), where X1 is TM channel 2 minus TM channel 3 multiplied by the ratio of TM channel 1 to TM channel 2; TSS = a + b(X1) + c(X2), where X1 is the ratio of TM channel 2 to TM channel 4 and X2 is the ratio of TM channel 3 to TM channel 5.

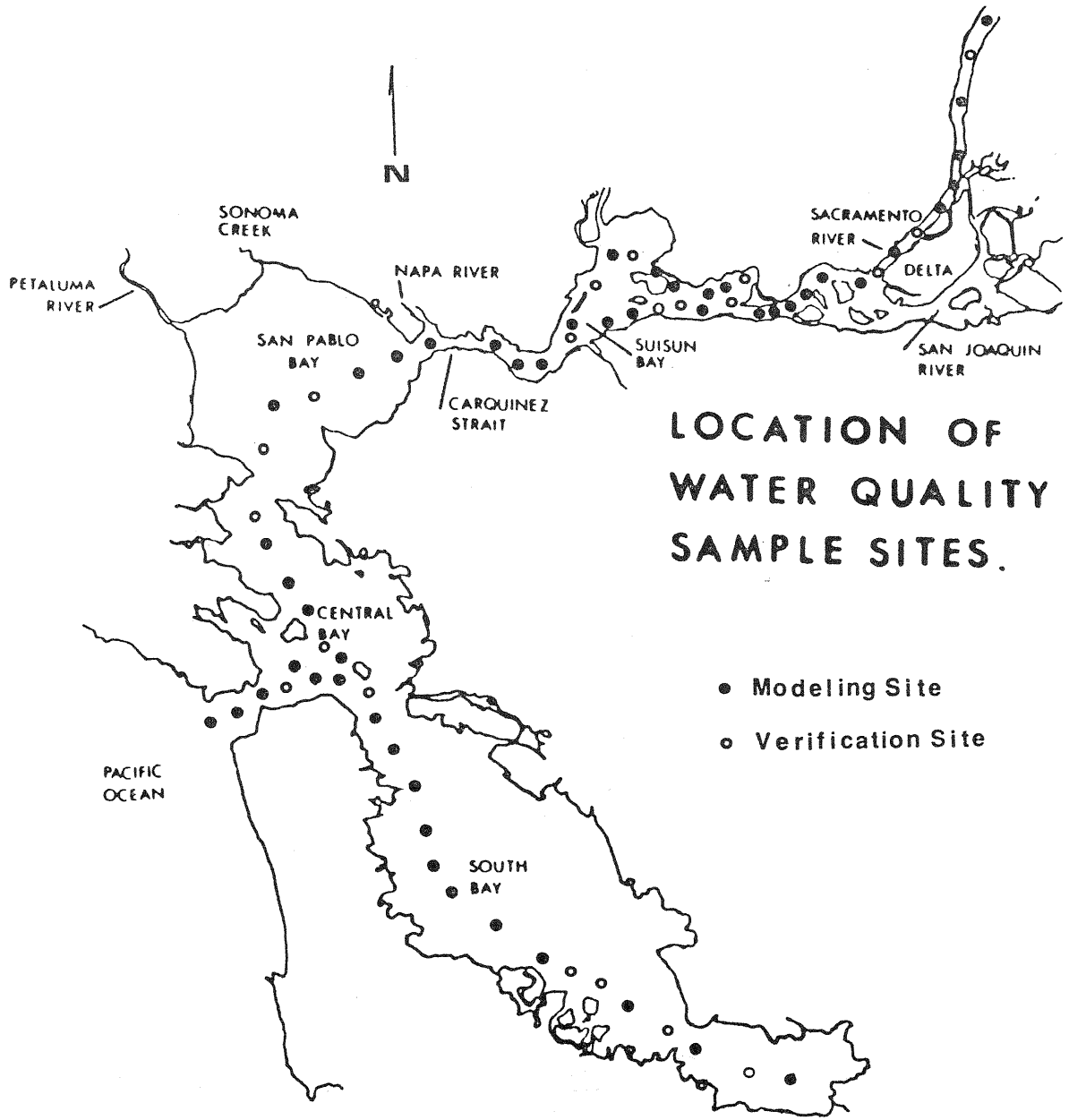

Figure 1. Location of surface sample sites on May 2, 1984. Scale is approximately 1:500,000.

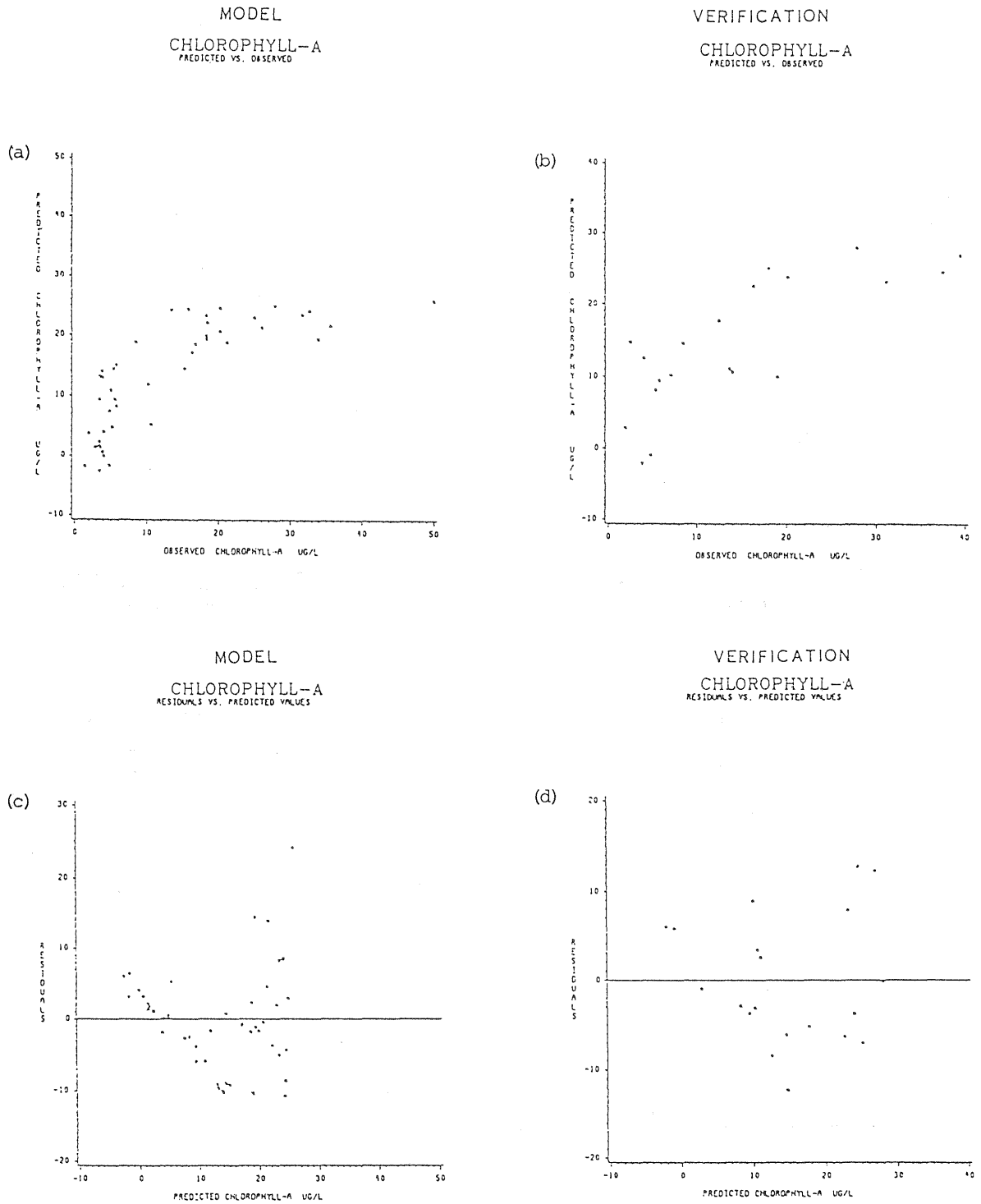

Figure 2. Chlorophyll a modeling (n=49) and verification (n=20) performance: predicted versus observed chlorophyll a concentrations for modeling (a) and verification (b); residuals versus observed chlorophyll a concentrations for modeling (c) and verification (d).

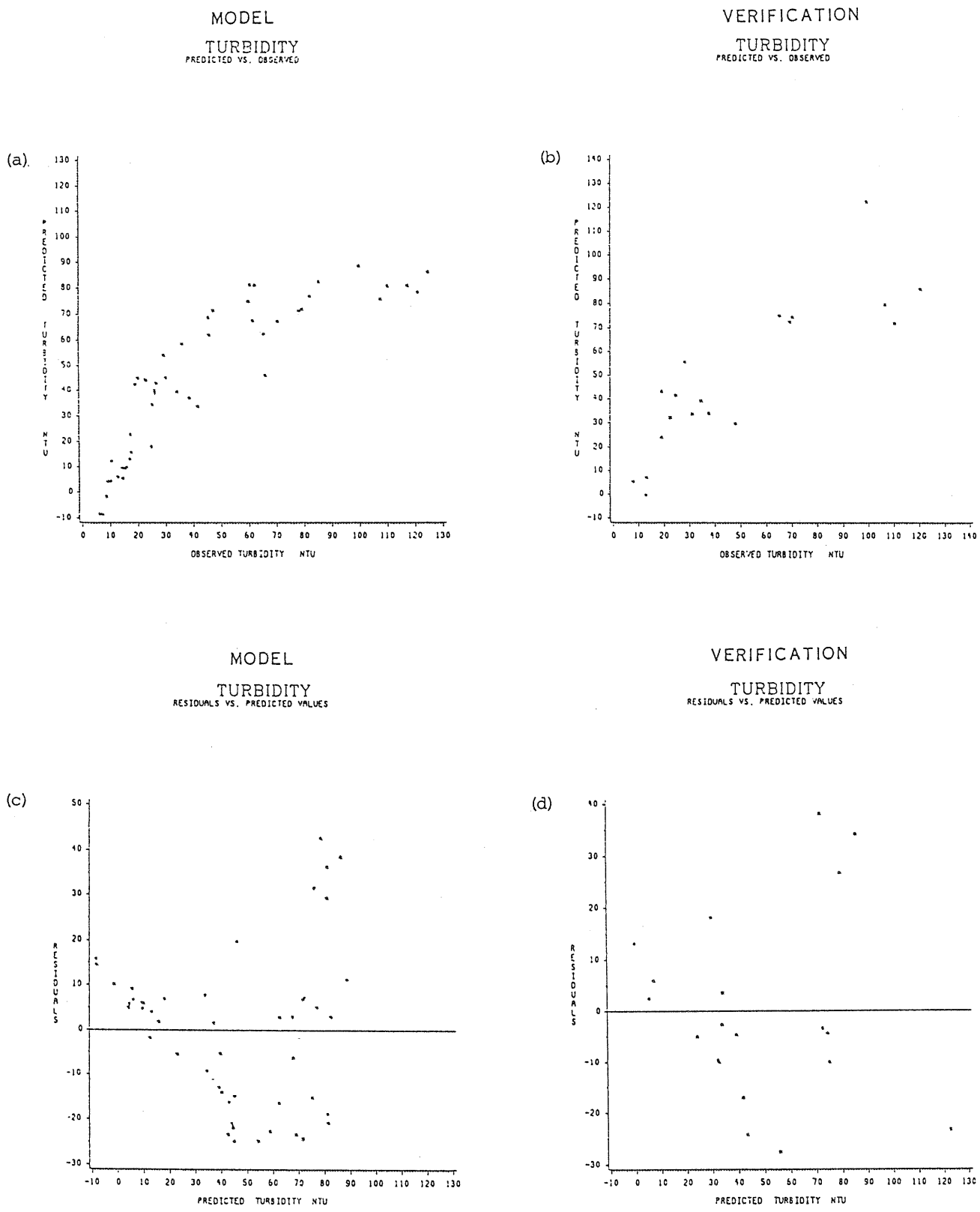

Figure 3. Turbidity modeling (n=49) and verification (n=20) performance: predicted versus observed turbidity concentrations for modeling (a) and verification (b); residuals versus observed turbidity concentrations for modeling (c) and verification (d).

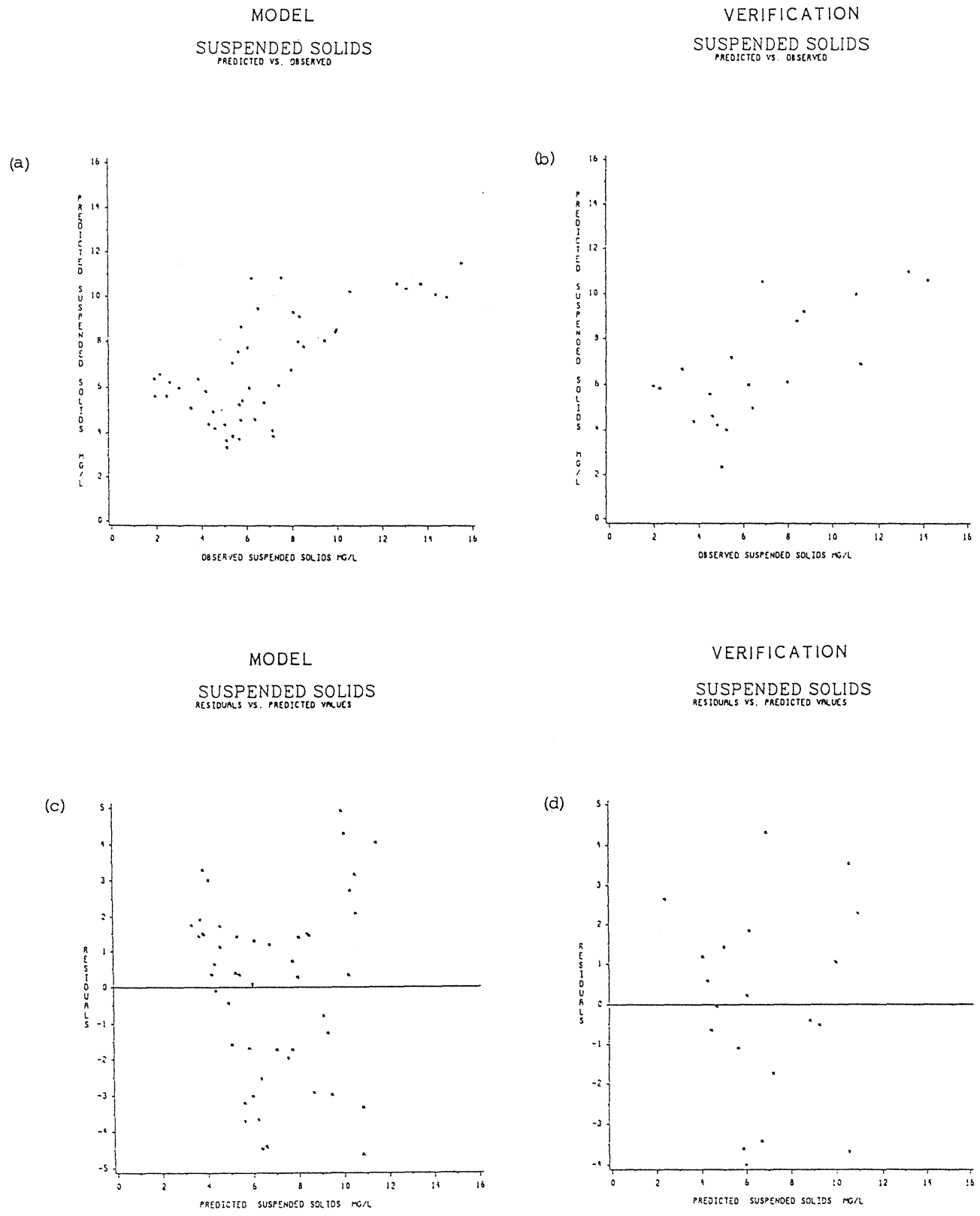

Figure 4. Suspended solids modeling (n=49) and verification (n=20) performance: predicted versus observed suspended solids concentrations for modeling (a) and verification (b); residuals versus observed suspended solids concentrations for modeling (c) and verification (d).

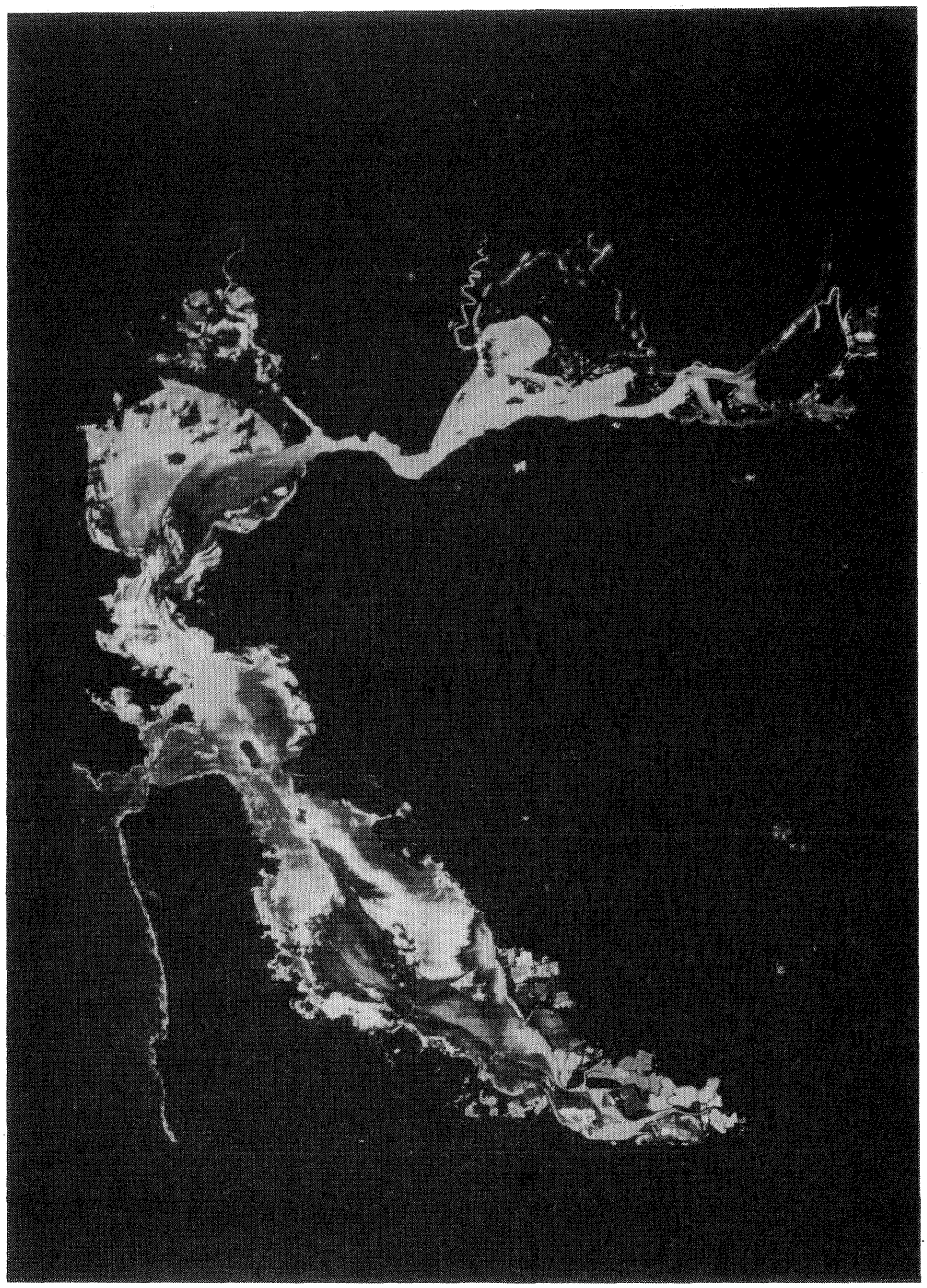

Figure 5a. Chlorophyll a predicted surface concentration map.

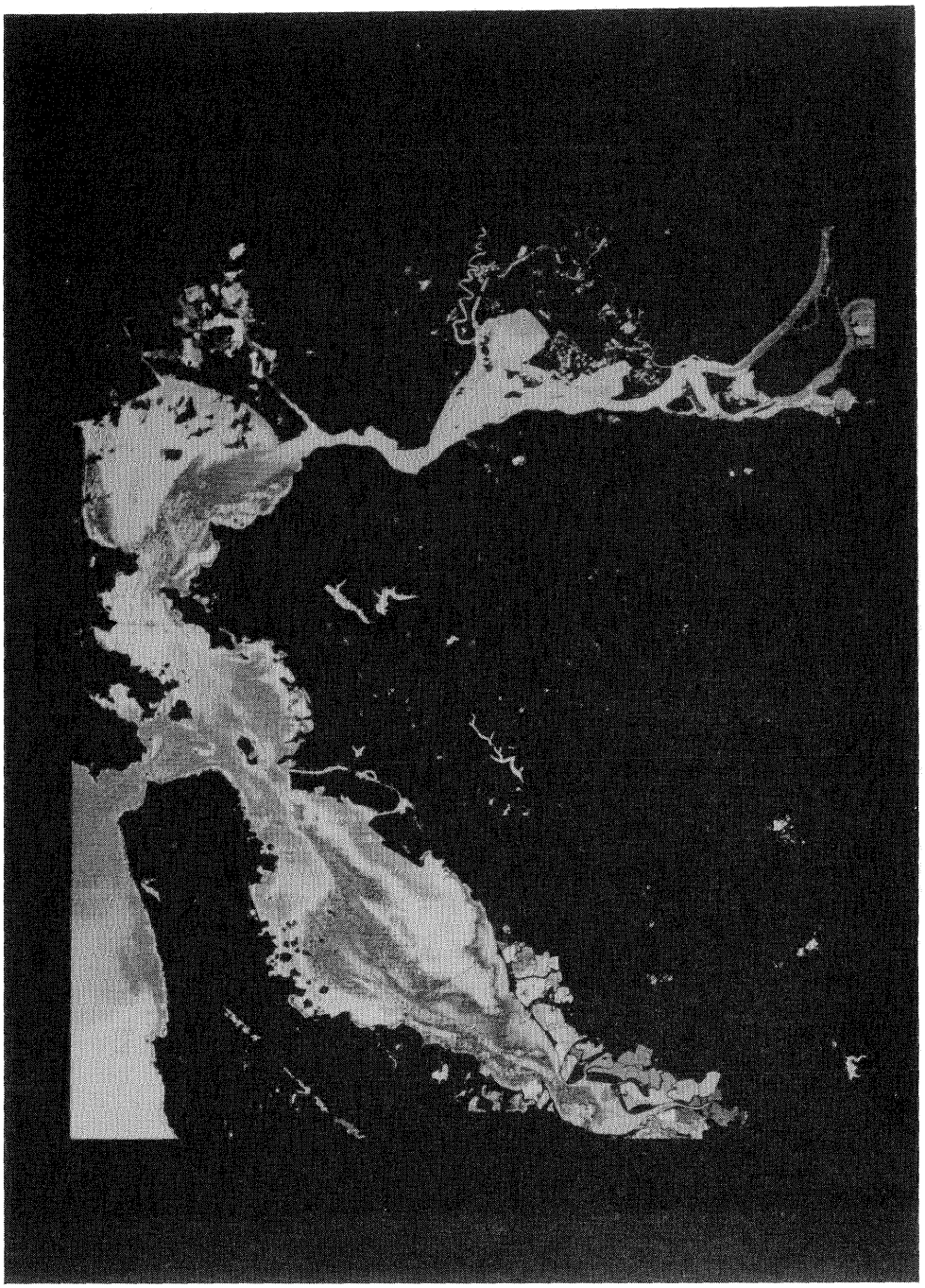

Figure 5b. Turbidity predicted surface concentration map.

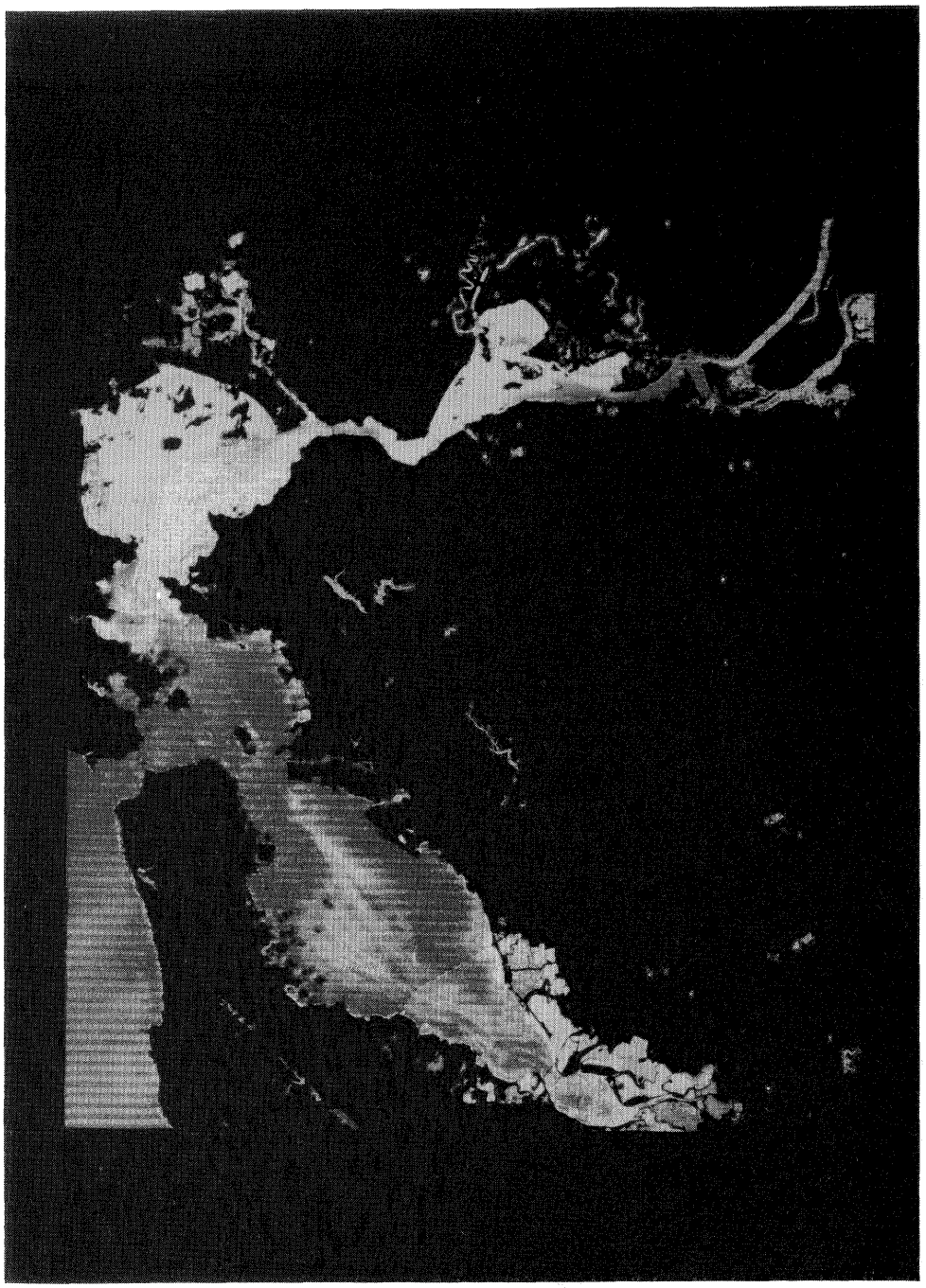

Figure 5c. Suspended solids predicted surface concentration map.